Dilute nanostructures built of dimers: Kinetic Monte Carlo study of Co on Cu(111)

Jolanta M. Rogowska
Institute of Experimental Physics, University of Wrocław, pl. M. Borna 9, 50-204 Wrocław, Poland
(Received 27 January 2010; revised manuscript received 18 June 2010; published 30 July 2010)

The growth of Co on Cu(111) at coverage 0.03 monolayer is studied by kinetic Monte Carlo simulations performed above temperature of dimer formation (20–21 K) in order to find a nanostructure composed primarily of dimers as an analog of the dilute nanostructure formed of monomers. Both of the nanostructures are stabilized by a long-range surface-state-mediated interaction between adatoms. In order to obtain the largest possible fraction of dimers the simulation procedure consists in deposition of adatoms at low temperature (7 K) and simulated annealing at higher temperatures. After 60–200 s of annealing at 21–22 K, about 87% of adatoms belongs to dimers. The dimers form dilute islands with a local hexagonal order and an average nearest-neighbor distance of 12.0(5) Å. The nanostructure in the dimer state is stable up to 200 K.

DOI: 10.1103/PhysRevB.82.035444 PACS number(s): 68.43.Hn, 68.43.Jk, 68.65.Cd

I. INTRODUCTION

Recent progress in scanning tunneling microscopy and other surface sensitive techniques reveals a rich variety of submonolayer structures grown on metal surfaces. The structure of metallic adlayer is determined by the interaction between adatoms and by the growth conditions. Three distinct interaction regimes with respect to the adsorbate separation can be distinguished: the direct electronic interactions at short separations, the electrostatic and elastic fields at larger separations, and the indirect oscillatory interactions at long separations.[1] Of particular interest are the long-range interactions mediated by the two-dimensional (2D) electron gas realized in the Shockley-type surface states of densely packed surfaces of noble metals. Recent experimental studies have shown that at low temperature and coverage the interactions stabilize new dilute nanostructures with average nearest-neighbor distance d a few times longer than an equilibrium adatom-adatom distance r_{eq}.[2] The value of d depends on adsorbate species and varies from 3.0 nm [for Ag(111)] to 1.2 nm [for the Cu (111) surface]. The dilute nanostructures have been observed experimentally[3–10] and modeled by kinetic Monte Carlo (KMC) simulations.[9–18] The nanostructures may be divided into two classes: (i) 2D superlattices with the long-range hexagonal order as Ce on Ag(111),[6,7,11] and on Cu(111),[9] (ii) 2D dilute islands with the weak local hexagonal order as Co,[5] Cu,[3–5,12] and Fe,[10,14] on the Cu(111) surface, as well as Co (Ref. 5) on the Ag(111) surface. The detailed discussion of inability of superlattice formation in most of considered systems can be found in Refs. 2, 5, 10–12, and 14. Besides 2D nanostructures, at a very low adatom coverage θ (about 0.002–0.005 monolayer (ML), adatoms have tendency to form dilute linear chains.[6–8,12–14] The dilute islands are observed at a coverage of about 30% lower than the saturation coverage, i.e., coverage sufficient to form a perfectly ordered superlattice made up only of monomers. The saturated coverage is equal to 0.01 ML for Ag(111) (Refs. 6, 7, and 11) and 0.048 ML for Cu(111).[14]

Experimental and theoretical investigations of the dilute nanostructures are restricted to a narrow temperature window between the temperature of single adatom diffusion T_{diff} and that of dimer formation T_D. The onset of dimer formation, defined in Ref. 5, corresponds to 10% of monomers having formed dimers and trimers after 2 min of annealing of a surface covered by 0.003 ML. A dimer situated among monomers is considered as a defect because the monomers adjusting their positions around the dimer destroy the local order of nanostructure.[6,7,9–11] The formation of dimers and bigger clusters has been studied for the following systems: Fe/Cu(111),[10] Ce/Ag(111),[11] Al/Al(111),[15] Cu/Cu(111),[15,16] Ag/strained Ag(111),[16–18] and Cu/Ag(111).[19,20] It has been shown[15–18] that substrate-mediated interactions may lead to sharp island-size distributions (with most of islands built of 2–3 adatoms) but there was no attempt to create a nanostructure built of dimers. The suggestion of the necessity of preparing such a nanostructure can be found in Ref. 20, where the influence of dimers on adatom motion in the Cu/Ag(111) system has been investigated. The aim of this work is to find, by kinetic Monte Carlo modeling, the conditions for spontaneous formation of nanostructure primarily made up of dimers as an analog of the above-mentioned nanostructure of monomers.

II. KMC MODEL

The interactions responsible for self-assembling of the metallic adatoms on the (111) surfaces of noble metals are mediated by a 2D electron gas realized in the Shockley-type surface states on the close packed surface of noble metals as well as by electrons of bulk metal.[8–10,15–18,21–24] The pair-interaction potential for the asymptotic adatom-adatom separation $r > \pi/q_F$ has been estimated theoretically[22] as

$$V(r) \approx -\varepsilon_F \left[\frac{2\sin(\delta_F)}{\pi}\right]^2 \frac{\sin(2q_F r + 2\delta_F)}{(q_F r)^2}, \qquad (1)$$

where q_F is the in-surface Fermi wave vector, δ_F is the adsorbate's scattering phase and ε_F is the Fermi energy. At intermediate distances $r_0 \approx 0.5$ nm the interplay between the elastic and electrostatic interactions leads to the existence of an attachment barrier V_0 of 20–60 meV, which prevents dimer formation and delays nucleation of island.[15–18] At distances shorter than r_0, the chemical bonding leads to dimer formation with a conventional bond length r_{eq} and bonding

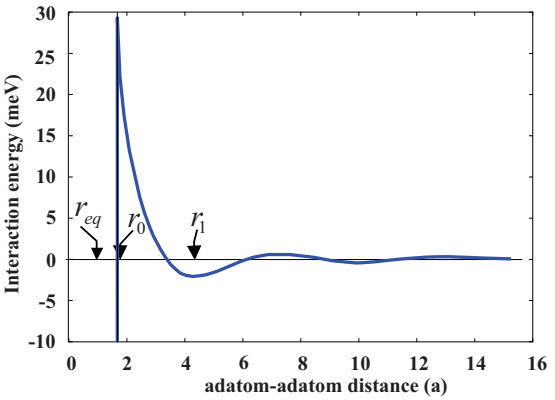

FIG. 1. (Color online) The pair-interaction energy between Co adatoms on Cu(111) incorporated in KMC simulations. Adatoms are separated by a distance r shown in the units of Cu(111) surface parameter $a=0.256$ nm. The distances indicated in the figure relate to the following energies: $V_{eq}(r_{eq})=-1181.74$ meV, $V_0(r_0)=29.60$ meV, and $V_1(r_1)=-2.01$ meV. For reasons of scale, on the energy axis the short-range interaction with the ordinary dimer energy V_{eq} is not shown. For $r<11a$ the curve is based on the energy values taken from Refs. 8 and 25 whereas for longer distances a fit based on Eq. (1) is used.

energy of the order of 1–2 eV. The Co-Co potential $V(r)$ applied in this work is shown in Fig. 1, where for $r<11a$ the curve is based on the energy values taken from Refs. 8 and 25, whereas for longer distances a fit based on Eq. (1) is used. The distances indicated in the figure expressed in the Cu(111) lattice parameter $a=0.256$ nm, are related to the following energies: the binding energy of a dimer $V_{eq}(r_{eg}=a)=-1181.74$ meV, the attachment barrier $V_0(r_0)=29.60$ meV, where $r_0=1.73a$; and the first minimum of the substrate mediated potential $V_1(r_1)=-2.01$ meV, where $r_1=4.36a$. The Co adatoms on Cu(111) have a magnetic moment[21] equal to 1.9 μ_B, where μ_B is the Bohr magneton. The magnetic interaction Co-Co is inexplicitly included in the pairwise potential $V(r)$.

The Cu(111) surface is represented as a hexagonal lattice of fcc and hcp hollow sites with the separation $a/\sqrt{3}$ between the nearest sites. The size of the simulation cell is $100a \times 111a$ with periodic boundary conditions. At every MC step an ith adatom performs a jump over a barrier ΔE^i to one of the nearest empty sites. The hopping rate of an event m is given by the Arrhenius law $h(m)=\nu_0 \exp(-\Delta E^i/k_BT)$, where T is the substrate temperature, k_B is the Boltzmann constant, and the attempt frequency is assumed to be $\nu_0=1 \times 10^{12}$ s^{-1}. The hopping barrier ΔE^i is calculated as the difference in the total adatom energy between the initial state (fcc or hcp site) and the transition state (bridge site)

$$\Delta E^i = E^i(\text{transition}) - E^i(\text{initial}). \tag{2}$$

The adatom energy E^i is divided into two parts. One is an ith adatom interaction with the substrate E^i_s and the other is a lateral interaction E^i_{lat} between the ith adatom and its neighbors, therefore $E^i=E^i_s+E^i_{lat}$. The magnitudes of the surface energy barriers ΔE^i_s for a single Co adatom on the Cu(111) surface are equal to 37 meV for fcc→hcp, and 36 meV for hcp→fcc jumps.[8,13,26] Although, in general, the interactions are not pairwise additive,[23,24] for a dilute submonolayer the assumption of their additivity is justified,[11,16] and then the lateral energy of the ith adatom energy is written as

$$E^i_{lat} = \sum_{r^{ij}=1}^{r_{cut}} V^{ij}(r^{ij}), \tag{3}$$

where the $V^{ij}(r^{ij})$ is a pair-interaction energy between the ith and jth adatoms separated by r^{ij}. For practical reasons the summation of E^{ij}_{lat} is performed up to the cutoff radius r_{cut} so that all of the remaining pair-interaction energy falls off to zero for $r^{ij}>r_{cut}$. In the systems where the interaction between adatoms is an oscillatory function of interatomic distance, the cut-off radius should not be selected in an arbitrary way. It was shown in Ref. 27 that the tendency of adatoms to self-assemble strengthens and weakens with the same periodicity vs. r_{cut} as the pair-interaction energy vs interatomic distance. For the Cu(111) surface the r_{cut} should be chosen from "neutral" cut-off radii: $11a$, $14a$, $17a$, or $20a$. At temperatures of 16–23 K the reasonable choice for r_{cut} is $14a=3.6$ nm.

The KMC simulates the Poisson processes and is performed according to the rejection-free method.[28] All possible diffusion events for a given configuration of adatoms are defined *a priori* and described by relative probabilities $w(m)=h(m)/R$, obtained from the hopping rates $h(m)$ weighted by a total rate of surface activity R. The total rate is given by $R=N_0h_0+\Sigma h(m)$, where N_0 is the number of adsorption sites, and the sum runs over all possible events except deposition, and h_0 is the deposition rate. The time interval between the events (δt) has a Poisson distribution $\delta t=-1/R \ln(1-Rr1)$, where $r1$ is a random number in the interval (0, 1). At every MC step, the event to take place is selected by a linear selection procedure.[29]

III. RESULTS

The KMC modeling simulates deposition and annealing of Co adatoms on the Cu(111) surface. Adatoms deposited below the temperature of adatom diffusion $T_{dif}=10-12$ K are randomly distributed on the surface. The small number of dimers and bigger clusters are a result of statistical growth. Atoms deposited on the top of a monomer (or a cluster) are allowed to descent and attach laterally the monomer. Moreover, an atom deposited inside the radius r_0 around a monomer slips to the potential well at r_{eq} and forms a dimer.

The randomly distributed monomers annealed at $T \geq T_{dif}$ self-organize into dilute islands with the local hexagonal structure. When the temperature of annealing is lower than that of dimer formation ($T_D=21-22$ K), the dilute islands primarily consist of monomers. For $T>T_D$ the dilute islands consist of monomers, dimers, trimers, and larger clusters. In order to maximize the number of dimers and minimize the number of trimers the annealing temperature should be close to T_D and the coverage should be lower than the saturation coverage. In this work the following procedure is applied: (i) deposition of 0.03 ML at a flux of 0.01 ML/s and temperature 7 K. (ii) Annealing the deposited adlayer at a tempera-

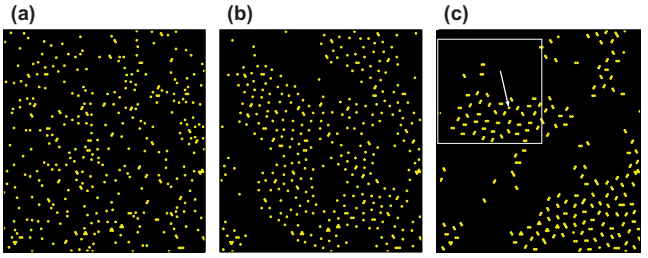

FIG. 2. (Color online) Snapshots of 0.03 ML of Co on the Cu(111) surface. The size of the simulation cell is $100a \times 111a$. (a) Random configuration of adatoms deposited at 7 K at a flux 0.01 ML/s. (b) The nanostructure made up of monomers ($T=16$ K, annealing time $t=500$ s). (c) The nanostructure composed of dimers ($T=22$ K, $t=140$ s). White arrow points at monomer trapped among dimers. The marked region is shown in Fig. 5.

ture below T_D, until adatoms self-organize into the nanostructure made of monomers. (iii) Annealing the deposited adlayer at a temperature T_D until the number of dimers reaches its maximum.

Figure 2 presents the snapshots of evolution of the simulated Co submonolayer. Figure 2(a) shows the submonolayer immediately after deposition at 7 K. At this temperature the adatom diffusion is frozen and adatoms are arranged randomly, where 73% of adatoms are in the form of monomers, 22% of dimers, 5% of trimers, and larger clusters. The random arrangement of adatoms, shown in Fig. 2(a), has been used as the initial configuration for annealing at $T=16-23$ K. The results for 16 K and 22 K are shown in Figs. 2(b) and 2(c), respectively. Because dimers (and larger clusters) do not diffuse at considered temperatures, the dimers nucleated during deposition can be found in Figs. 2(a)–2(c) in the same positions. At 16 K adatoms rearrange into a dilute percolating island. The island consists mainly of monomers (72%). An average separation between monomers (precisely defined in Ref. 12) equals $4.6(1)a$. About 63% of adatoms are in fcc sites. Monomers in the island are locally mobile and instantaneously change their position in a wide and shallow potential well around r_1 (Fig. 1). One can say that the island is in a "dilute liquid" state. At $T \geq 20$ K some adatoms have the kinetic energy large enough to form dimers in a reasonable time. Figure 2(c) presents a nanostructure containing mostly dimers as obtained by simulated annealing at 22 K. The dimers form dilute islands with a weak local hexagonal order and an average mutual distance of $4.7(2)a$. Here, the 1% of adatoms is in the form of monomers, 87% of dimers, 12% of trimers, and larger clusters. About 61% of adatoms are in fcc sites. The white arrow points at monomer trapped among dimers. The trapped monomer has no chance to meet another monomer and form a dimer but it would end up us a part of a new linear trimer. Such a favorable attachment from the ends of a dimer was discussed in Refs. 8, 16, and 30. The tendency to linear chain formation seems to be a general feature of systems with oscillatory interactions between adatoms.

The KMC code (developed by the author[12]) enables one to observe adatoms' movement. At temperature of 16–23 K monomer diffuses freely on the clean surface. Dimer can carry out only a localized nondiffusive motion. It is a rotational motion around the central atom in the hexagonal cell of six substrate atoms. Individual atoms can jump over the transition (bridge) sites taking the dimer through fcc-fcc, fcc-hcp, and hcp-hcp configurations. The dimer intracell motion has been discussed for Cu/Ag(111),[19,20] Al/Al(111),[31] and Cu/Cu(111) (Ref. 32) systems. The binding energy of Co dimer (1.2 eV) prevents its dissociation and out-of-the-cell motion. As it has been observed in Ref. 20, the rotation of dimer is strongly influenced by neighboring dimers and monomers. Problem of dimmers mobility is out of the scope of this work. The trimers are immobile in the considered range of temperatures.

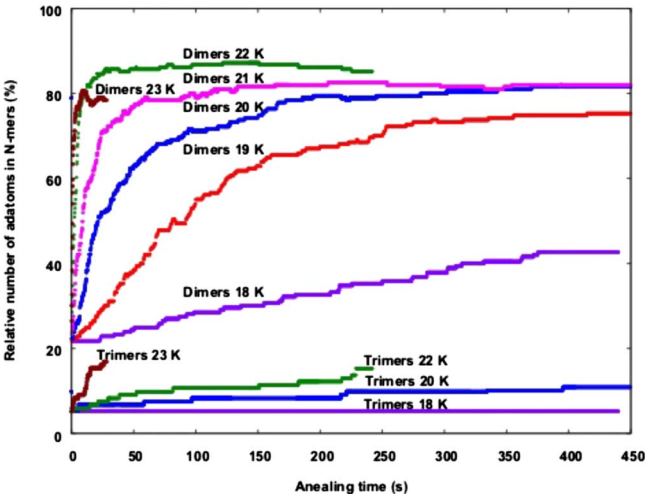

FIG. 3. (Color online) Relative number of adatoms in the form of dimers and trimers as a function of annealing time. The annealing temperature is a parameter of the curve. For clarity, curves for trimers at $T=19$ and 21 K are not shown.

Figure 3 presents the relative number (in %) of adatoms in the form of dimers (N_{dim}) and trimers (N_{trim}) as a function of annealing time t, at temperatures 18–23 K. It allows to find the temperature leading to a nanostructure composed of dimers with the lowest possible number of monomers and trimers. For clarity, the curves $N_{trim}(t)_T$ for $T=19$ and 21 K are not shown. The $N_{\mathrm{dim}}(t)_T$ initially increases very fast, reaches a flat maximum and then slowly decreases. The temperature 23 K is already too high, because the $N_{\mathrm{dim}}(t)$ abruptly decreases as a result of nucleation of trimers. The $N_{\mathrm{dim}}(t)_T$ has maximal value at $T=22$ K and $t \cong 140$ s.

At a given coverage and $T > T_D$, the probability of dimer formation depends on the number of active monomers. Only the active monomers are able to meet another active monomer and nucleate a dimer. Monomers trapped among dimers do not participate in nucleation of dimers. Formation of dilute island made of dimers can be divided into two stages. In the first stage there are plenty of active monomers and the dimers are nucleated very frequently. It is the stage of dimer formation, where the processes of monomer self-assembling (0–1 s) into a dilute island as well as formation of dimers (0–40 s) take place at the same time. (The numbers in the parenthesis relate to time of annealing at 22 K.) At the second stage ($t > 40$ s), the active monomers are nearly used up and dimer formation is hindered. The remaining active monomers are located at island edges. They diffuse along the

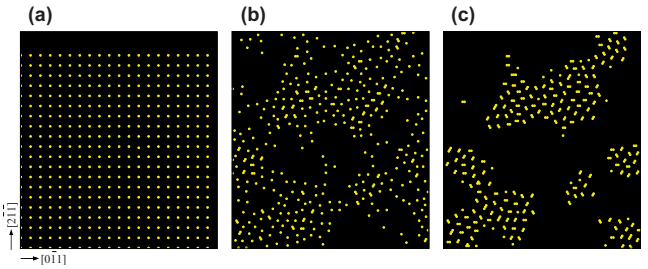

FIG. 4. (Color online) Snapshots of 0.031 ML of Co on the Cu(111) surface. The size of the simulation cell is $100a \times 111a$. (a) Lattice of monomers taken as initial configuration for annealing at 20 K. The monomers are located in fcc sites. In superstructure matrix notation the lattice can be described as fcc(111)-$\begin{bmatrix} 5 & 0 \\ 2 & 6 \end{bmatrix}$. (b) First stage: A dilute percolating island formed after 8 s of annealing, where 73% of adatoms is in the form of monomers and 27% in the form of dimers. (c) Second stage: dilute islands formed after 270 s of annealing, where 6.5% of adatoms is in the form of monomers, 86% is in the form of dimers, and 7.5% is in the form of trimers.

edges and eventually form dimers or trimers. The trapped monomers are also a source of trimers; therefore this stage can be called the stage of trimer formation. Because trimers are nucleated at the cost of dimers, at the end of this stage the number of dimers decreases.

Figure 4 illustrates the stages of dilute islands formation at $T=20$ K. Here, in contrast to the previous simulations, a regular lattice of monomers located on fcc sites is taken as the initial configuration of adatoms. Now, annealing starts without dimers. Due to the statistical process of dimer formation the dimers nucleated at the first stage are distributed randomly [Fig. 4(b)]. The barrier for diffusion of monomers is much lower than the energy barrier for dimer formation; therefore monomers have enough time to adjust their position around the newly formed dimer. After 8 s of annealing, the dilute island of monomers containing also some dimers is completed and only 63% of adatoms are located in fcc sites. The dimers, formed at the beginning of the first stage, act as centers of aggregation for monomers. With increasing number of dimers the dilute island shrinks. As it is seen in Fig. 4(c), monomers have abandoned the regions devoid of dimers and the shrinking island has been divided into smaller ones. Figure 4(c) presents dimer islands at the stage of trimer formation, where few monomers trapped among dimers and several active monomers at island edges can be seen.

In order to show in which way the island built of dimers grows, the map of lateral energy of the test monomer is presented in Fig. 5. The energy map can help answer the question "how do dimers influence the monomer motion?" The mapped region relates to the fragment of the submonolayer presented in Fig. 2(c) that is marked by a square. Disks and diamonds represent adatoms and vacant sites, respectively. The submonolayer has additionally been annealed by the next 6 s in order to show formation of a trimer from a trapped monomer and its neighboring dimer. The white arrow points at the new trimer. The light gray sites (orange color in the online version) of the map depict the attachment barriers. The dark gray sites (violet color in the online version) represent regions with a weak repulsion that the test

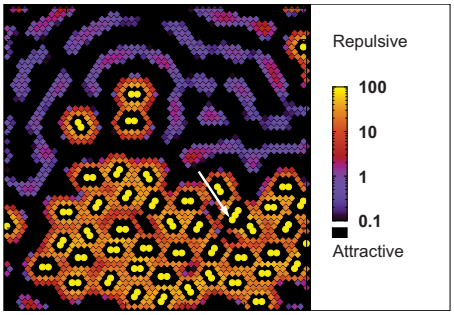

FIG. 5. (Color online) Map of lateral energy of a test adatom that was placed in the vacant fcc sites marked by diamonds. Size of the mapped region is $50a \times 50a$. The map relates to the fragment of Fig. 2(c) marked by a square, that was additionally annealed at 22 K by 6 s. The disks represent adatoms. They form an island, which consists of dimers and one linear trimer (pointed by arrow). Monomer pointed by the arrow in Fig. 2(c) now is a part of this trimer. The map shows also three dimers that do not belong to the island. One of them is in hcp-hcp configuration, two of them in fcc-fcc configurations. The repulsive energy at fcc sites is presented in the logarithmic scale with the base 10. The regions of attractive energy are black, independent of the energy value.

adatom can overcome at 22 K. The black sites show regions with an attractive lateral energy of the test adatom. For example, the three-site black ribbon nearby the island relates to the potential well at the first minimum of oscillatory interactions between the test adatom and dimers forming the island. The probability of finding the test adatom in regions with repulsion is very low. However, the adatom can easily diffuse along the black ribbons, where attractive interactions exist. If two monomers are attracted into this region they form sooner or latter a new dimer. The newly formed dimer is located at the edge of the island at a distance of $4-6a$ from neighboring dimers. In this way, the island made of dimers grows until the number of active monomers goes to zero. Looking closely one can distinguish the dimers in fcc-fcc and fcp-hcp configurations. For example, at an upper left-hand quarter of the map, the single dimer near the island is in the fcc-fcc configuration.

At this point, the thermal stability of the nanostructure in the dimer state should be addressed. The nanostructure presented in Fig. 2(c) remains almost unchanged after annealing at 200 K for $t=1 \times 10^{-4}$ s. In the first picoseconds, several remaining monomers join dimers to form trimers, by successive nanosecond the linear trimers become compact. Later on, the values of $N_{\mathrm{dim}}=86\%$ and $N_{trim}=14\%$ do not change. Therefore, in the presented model the nanostructure is stable up to 200 K. A similar result has been obtained by the molecular dynamic simulation[33] for an ellipsoidal corral artificially constructed from Co dimers on Cu(111), namely, the corral has been reported to be stable up to 200 K. With a local hexagonal order in dimers arrangement and dimer rotating only by intracell motion, the dilute island built of dimers ($T=21-200$ K) resembles a "dilute 2D amorphous crystal" with a higher density and rigidity "than dilute 2D liquid" (dilute island made of monomers). It should be mentioned that the collective adatom movements (for example, a concerted sliding of dimer), are neglected in the KMC

model. The collective movements can be responsible for the out-of-the-cell dimer motion and nucleation of a tetramer. However, the tetramer formation is very unlikely at $T \leq 200$ K because the dimer is additionally pined up by long-range substrate-mediated interactions with neighboring dimers.

IV. DISCUSSION AND SUMMARY

The kinetic Monte Carlo simulation demonstrates that the surface-state mediated long-range interaction between Co adatoms on the Cu(111) surface can lead to their self-assembling into two kinds of dilute islands, namely, the islands containing monomer or dimer basis. The islands have a local hexagonal order with the mutual distance between the monomers (or dimers) close to the first minimum of the long-range potential. The possibility of the existence of a dilute nanostructure in the dimer state concerns also other metallic submonolayers deposited on noble metal surfaces. For example, the author has obtained such a nanostructure for Cu on the Cu(111) surface at 20–21 K (unpublished). In order to create a nanostructure primarily containing the dimers the submonolayer deposited at a very low temperature ($T < T_{dif}$) has to be annealed at the temperature of dimer formation. If at this temperature the diffusing monomers are effectively attracted by the first potential well of substrate-mediated potential around dimers, the island made up of dimers will grow. Once formed, the nanostructure is stable as long as dimers do not perform out-of-the-cell movements leading to nucleation of bigger clusters. Within assumptions underlying the presented model, the KMC simulation shows that, for the Co/Cu(111) system, the nanostructure is stable up to 200 K.

The thermal stability of the dimer nanostructure, together with its magnetic properties, may stimulate undertaking new experiments, for example an investigation of the existence of magnetic hysteresis in such a system. The magnetic coupling mediated by surface-state electrons is also an oscillatory function of distance between adatoms.[21] The nearest Co neighbors (at a distance r_{eq}) are coupled ferromagnetically whereas next-nearest Co neighbors (at a distance $4-5r_{eq}$) are coupled antiferromagnetically. Magnetization response to the external magnetic field for a dilute nanostructure composed of monomers separated by $4.4r_{eq}$ that are ferromagnetically coupled [for example, a dilute Cr island on Cu(111)], has recently been simulated by KMC.[34] The system reveals a hysteresislike behavior at 1–3 K. For the Co/Cu(111) nanostructure in the dimer state, where the magnetic interactions are hundred times stronger,[21] the hysteresis should be observed at a much higher temperature.

ACKNOWLEDGMENTS

I gratefully thank V. S. Stepanyuk and A. N. Baranov for providing me the tabularized DFT Co-Co interaction potential (Ref. 8) used in the KMC simulations.

[1] A. Kiejna and J. M. Rogowska, in *Recent Developments in Vacuum Science and Technology*, edited by J. Dabrowski (Research Signpost, Kerala, 2003), p. 133.
[2] H. Brune, in *Single Molecules at Surfaces*, edited by F. Rosei, P. Grütter, and W. Hofer (Springer, New York, 2006), p. 247.
[3] J. Repp, Ph.D. thesis, Free University of Berlin, 2002.
[4] J. Repp, F. Moresco, G. Meyer, K. H. Rieder, P. Hyldgaard, and M. Persson, Phys. Rev. Lett. **85**, 2981 (2000).
[5] N. Knorr, H. Brune, M. Epple, A. Hirstein, M. A. Schneider, and K. Kern, Phys. Rev. B **65**, 115420 (2002).
[6] F. Silly, M. Pivetta, M. Ternes, F. Patthey, J. P. Pelz, and W. D. Schneider, Phys. Rev. Lett. **92**, 016101 (2004).
[7] F. Silly, M. Pivetta, M. Ternes, F. Patthey, J. P. Pelz, and W. D. Schneider, New J. Phys. **6**, 16 (2004).
[8] V. S. Stepanyuk, A. N. Baranov, D. V. Tsivlin, W. Hergert, P. Bruno, N. Knorr, M. A. Schneider, and K. Kern, Phys. Rev. B **68**, 205410 (2003).
[9] N. N. Negulyaev, V. S. Stepanyuk, L. Niebergall, P. Bruno, M. Pivetta, M. Ternes, F. Patthey, and W. D. Schneider, Phys. Rev. Lett. **102**, 246102 (2009).
[10] N. N. Negulyaev, V. S. Stepanyuk, L. Niebergall, P. Bruno, W. Auwärter, Y. Pennec, G. Jahnz, and J. V. Barth, Phys. Rev. B **79**, 195411 (2009).
[11] N. N. Negulyaev, V. S. Stepanyuk, L. Niebergall, W. Hergert, H. Fangohr, and P. Bruno, Phys. Rev. B **74**, 035421 (2006).
[12] J. M. Rogowska and M. Maciejewski, Phys. Rev. B **74**, 235402 (2006).
[13] N. N. Negulyaev, V. S. Stepanyuk, W. Hergert, H. Fangohr, and P. Bruno, Surf. Sci. **600**, 58 (2006).
[14] J. Hu, B. Teng, F. Wu, and Y. Fang, New J. Phys. **10**, 023033 (2008).
[15] A. Bogicevic, S. Ovesson, P. Hyldgaard, B. I. Lundqvist, H. Brune, and D. R. Jennison, Phys. Rev. Lett. **85**, 1910 (2000).
[16] K. A. Fichthorn, M. L. Merrick, and M. Scheffler, Phys. Rev. B **68**, 041404(R) (2003).
[17] K. A. Fichthorn and M. Scheffler, Phys. Rev. Lett. **84**, 5371 (2000).
[18] K. A. Fichthorn, M. L. Merrick, and M. Scheffler, Appl. Phys. A: Mater. Sci. Process. **75**, 17 (2002).
[19] K. Morgenstern, K. F. Braun, and K. H. Rieder, Phys. Rev. Lett. **93**, 056102 (2004).
[20] K. Morgenstern and K. H. Rieder, New J. Phys. **7**, 139 (2005).
[21] V. S. Stepanyuk, L. Niebergall, R. C. Longo, W. Hergert, and P. Bruno, Phys. Rev. B **70**, 075414 (2004).
[22] P. Hyldgaard and M. Persson, J. Phys.: Condens. Matter **12**, L13 (2000).
[23] P. Hyldgaard and T. L. Einstein, Europhys. Lett. **59**, 265 (2002).
[24] P. Hyldgaard and T. L. Einstein, Surf. Sci. **532-535**, 600 (2003).
[25] V. S. Stepanyuk and A. N. Baranov (private communication).
[26] J. A. Stroscio and R. J. Celotta, Science **306**, 242 (2004).
[27] J. M. Rogowska, Appl. Surf. Sci. **254**, 4370 (2008).
[28] K. A. Fichthorn and W. H. Weinberg, J. Chem. Phys. **95**, 1090 (1991).
[29] U. Burghaus, J. Stephan, L. Vattuone, and J. M. Rogowska,

A Practical Guide to Monte Carlo Simulations and Classical Molecular Dynamics Simulations: An Example Booklet (Nova Science, New York, 2006), p. 77.
[30] J. M. Rogowska, Vacuum **45**, 297 (1994).
[31] A. Bogicevic, P. Hyldgaard, G. Wahnström, and B. I. Lundqvist, Phys. Rev. Lett. **81**, 172 (1998).
[32] J. Repp, G. Meyer, K. H. Rieder, and P. Hyldgaard, Phys. Rev. Lett. **91**, 206102 (2003).
[33] V. S. Stepanyuk, N. N. Negulyaev, L. Niebergall, R. C. Longo, and P. Bruno, Phys. Rev. Lett. **97**, 186403 (2006).
[34] A. S. Smirnov, N. N. Negulyaev, W. Hergert, A. M. Saletsky, and V. S. Stepanyuk, New J. Phys. **11**, 063004 (2009).